Journal of Chromatography B 1242 (2024) 124188

Contents lists available at ScienceDirect

Journal of Chromatography B

journal homepage: www.elsevier.com/locate/jchromb

Improving the intestinal lipidome coverage in a gnotobiotic mouse model using UHPLC-MS-based approach through optimization of mobile phase modifiers and column selection

Habiba Selmi [a], Alesia Walker [a,*], Laurent Debarbieux [b], Philippe Schmitt-Kopplin [a,c]

[a] Research Unit Analytical BioGeoChemistry, Helmholtz Zentrum München, Neuherberg, Germany
[b] Institut Pasteur, Université Paris Cité, CNRS UMR6047, Bacteriophage Bacterium Host, Paris, France
[c] Chair of Analytical Food Chemistry, Technical University of Munich, Freising, Germany

ARTICLE INFO

Keywords:
Non-targeted lipidomics
Mobile phase modifiers
Hybrid surface technology
Oligo-Mouse-Microbiota

ABSTRACT

Lipidomics is focusing on the screening of lipid species in complex mixtures using mass spectrometry-based approaches. In this work, we aim to enhance the intestinal lipidome coverage within the Oligo-Mouse-Microbiota (OMM^{12}) colonized mouse model by testing eight mobile phase conditions on five reversed-phase columns. Our selected mobile phase modifiers included two ammonium salts, two concentrations, and the addition of respective acids at 0.1 %. We compared two columns with hybrid surface technology, two with ethylene bridged hybrid technology and one with core–shell particles. Best performance was attained for standards and intestinal lipidome, using either ammonium formate or acetate in ESI(+) or ammonium acetate in ESI (−) for all column technologies. Notably, a concentration of 5 mM ammonium salt showed optimal results for both modes, while the addition of acids had a negligible effect on lipid ionization efficiency. The HST BEH C18 column improved peak width and tailing factor parameters compared to other technologies. We achieved the highest lipid count in colon and ileum content, including ceramides, phosphatidylethanolamines and phosphatidylcholines, when using 5 mM ammonium acetate in ESI(−). Conversely, in ESI(+) 5 mM ammonium formate demonstrated superior coverage for diacylglycerols and triacylglycerols.

1. Introduction

Over the past decade, omics-based technologies; genomics, transcriptomics, metabolomics, and proteomics, have played a pivotal role in advancing biomarker discovery [1]. Recently, lipidomics, a specific metabolomics branch for lipid analysis, has emerged to comprehensively profile the molecules in biological samples [2,3]. Lipids are crucial molecules due to their integral role in various biological processes. Functioning as major constituents of cell membranes, they also serve as energy reservoirs, signaling mediators and facilitators of cellular interactions [4]. Numerous studies have underscored the link between disruption in lipids metabolism and a wide spectrum of diseases, including cardiovascular diseases, type 2 diabetes, obesity, and cancer [3,5,6]. Accumulating evidence suggests a potential association between perturbations in gut microbiota composition and the development of gastrointestinal diseases [7]. Given the high diversity of microbial lipids within the intestinal tract, they play crucial roles in various biological processes and can significantly impact host health and disease. Recent studies have highlighted the critical role of microbial-derived lipids in modulating host immune responses, particularly in the context of gut inflammation, and in maintaining intestinal homeostasis [8–10]. Lipids are diverse molecules in both their structures and functions [4]. They can be divided into eight main categories according to the LIPID MAPS classification and each category can be further

Abbreviations: BMP, Bismonoacylglycerophosphate; HexCer, Hexosylceramide; CE, Cholesteryl ester; Cer, Ceramide; CL, Cardiolipin; CoQ, Coenzyme Q; DG, Diacylglycerol; DG ether, Ether-linked diacylglycerol; DGDG, Digalactosyldiacylglycerol; LPC, Lysophosphatidylcholine; LPE, Lysophosphatidylethanolamine; MGDG, Monogalactosyldiacylglycerol; MGDG, ether, Ether-linked monogalactosyldiacylglycerol; NAGly, N-acyl glycine; NAGlySer, N-acyl glycyl serine; NAOrn, N-acyl ornithine; PA, Phosphatidic acid; PC, Phosphatidylcholine; PG, Phosphatidylglycerol; PG, ether, Ether-linked phosphatidylglycerol; PE, Phosphatidylethanolamine; PE ether, Ether-linked phosphatidylethanolamine; PI, Phosphatidylinositol; PI-Cer, Oxidized ceramide phosphoinositol; PS, Phosphatidylserine; SE, Steryl ester; ST, Sterol lipid; TG, Triacylglycerol.

* Corresponding author.
E-mail address: alesia.walker@helmholtz-munich.de (A. Walker).

https://doi.org/10.1016/j.jchromb.2024.124188
Received 26 March 2024; Received in revised form 21 May 2024; Accepted 30 May 2024
Available online 14 June 2024

divided into one or multiple subclasses [11,12]. Therefore, the development of advanced analytical techniques for lipid profiling remains ongoing, in order to assess their complex role more precisely in various physiological and pathological processes.

Targeted and non-targeted lipidomics are valuable approaches, when combined with liquid chromatography (LC) coupled to mass spectrometry (MS), it becomes a powerful tool for the comprehensive analysis of lipids. Reversed-phase LC (RPLC), normal-phase, hydrophilic interaction liquid chromatography, and supercritical fluid chromatography are among the widely employed chromatographic methods for lipid analysis [13]. Of these, RPLC columns packed with octadecyl (C18)-modified sorbents are accounting for over 70 % of columns used in reported studies [13–15]. This method has been proven to be effective in analyzing lipids in complex mixtures, relying on differences in lipophilicity defined by the carbon chain and number of double bonds [16,17]. RPLC columns used in lipidomics vary in column chemistry, particle size, or column length (typically 100 mm × 2.1 mm) [18]. While RPLC-MS-based setups have demonstrated the capability to analyze several hundreds of lipids, the detection of phosphatidic acids (PA) and phosphatidylserines (PS) remains challenging. The elution profiles of these lipid classes often exhibit broad peaks, a consequence of their interactions through phosphorylated or carboxylated head group functions with the metal surface of the column and injector [19]. To overcome these challenges and enhance both chromatographic peak shape and lipid coverage, various studies have explored modifications of either the mobile or stationary phase. One method involves adding chelators (phosphoric acid, citric acid and ethylenediaminetetraacetic acid) into the mobile phase or introducing an embedded carbamate group in the bonded phase ligand of octyl (C8) or C18 stationary phases [20–24]. Recent columns were developed using a hybrid surface technology (HST) applied to the metal substrates. This material, based on ethylene-bridged siloxane polymers, improved the detection of nucleotides, phosphopeptides, and lipids [25–27]. Furthermore, the choice of mobile phase modifiers remains a crucial parameter in enhancing separation, ionization, and detection of lipid species in LC-MS analysis [28]. Various combinations have been tested, using mostly 10 millimolar of ammonium formate or ammonium acetate with or without 0.1 % acetic or formic acid [29–34].

We employed both targeted and non-targeted approaches to analyze the intestinal lipidome of the isobiotic OMM^{12} mice [35]. These animals (axenic C57bl6 mice) are colonized by a consortium of twelve bacterial species spanning the five main phyla of murine intestinal bacteria and is a well-established tool recognized for its sustainable and reproducible intestinal bacterial content [36]. This model ensures a stable bacterial community for long-term mouse experiments making it invaluable for investigating host-microbe interactions by −omics approaches [37]. Given that a subset of lipid species, including those derived from the gut microbiota, has been shown to modulate immune responses and other biological processes, it is crucial to profile the intestinal lipidome to gain a better understanding of their implications in health.

In this study, we used intestinal content samples from OMM^{12} mice to conduct a thorough comparison of five RPLC columns with different materials for lipid analysis. Specifically, we assessed the performance of two HST Acquity UPLC columns (HSS T3 HST and BEH C18 HST), comparing them with the conventional Acquity UPLC columns (BEH C18 and BEH C8) and one core–shell particle column (Cortecs C18). Key chromatographic parameters such as peak width and tailing factor were defined and employed to compare the performance of these technologies. Furthermore, we extended our analysis beyond stationary phase evaluation and studied the influence of various mobile phase modifiers on lipid ionization. Exploring eight combinations of additives commonly used in lipidomics studies, with concentrations of 5 and 10 mM, we established several parameters to assess the impact of mobile phase modifiers on ionization efficiency for standards and biological samples. We evaluated peak areas and intensities of common lipid species in intestinal samples across the buffer conditions. Additionally, we compared the overall number of detected and annotated features for each mobile phase combination to explore the OMM^{12} intestinal lipidome.

2. Materials and methods

2.1. Reagents and materials

Acetonitrile (ACN), isopropanol (iPrOH), and methanol (MeOH) of LC-MS grade, same as methyl-*tert*-butyl ether (MTBE) of HPLC quality, were procured from Merck KGaA (Lichrosolv®, Darmstadt, Germany). Milli-Q water (H_2O) was obtained from the Milli-Q Integral Water Purification System (Billerica, MA, United States of America). Ammonium acetate (5 M, AmAc) and ammonium formate (10 M, AmF) were sourced from Merck KGaA, Darmstadt, Germany. Acetic and formic acid (LC-MS grade) were purchased from Fisher Scientific (Honeywell Fluka™, Hannover, Germany). A total of 140 lipid standards, comprising fatty acyls, glycerophospholipids, sphingolipids and other lipid classes, were acquired from various suppliers: Avanti Polar Lipids (Birmingham, AL, USA), Cayman Chemicals (Biomol, Hamburg, Germany), and Sigma–Aldrich (Sigma–Aldrich GmbH, Taufkirchen, Germany), as summarized in Table S1 and Table S3. Stock solutions were prepared at an initial concentration of 1 mg/mL in MeOH and subsequently diluted with ACN/iPrOH/H_2O (65/30/5) to a final concentration of 0.001 mg/mL for most of the standard mixtures and 0.0001 mg/mL for fatty acyl derivatives. Stable isotope-labeled internal standards (stock solution in MeOH, 1 mg/mL) were spiked at a final concentration of 0.001 mg/mL in blanks constituted of ACN/iPrOH/H_2O (65/30/5) and biological samples, and measurements were conducted in triplicates only for spiked blanks.

2.2. Sample preparation of ileal and colonic contents from OMM^{12} mice

Ten C57Bl/6J OMM^{12} mice aged of seven to nine weeks (bred in the gnotobiotic animal facility in accordance with Institut Pasteur guidelines and European recommendations under protocols approved by the National Ethics Committee APAFIS#26874-2020081309052574 v1), were used to collect intestinal content from both ileum and colon sections, taken aseptically. Lipid extraction of the intestinal content from colonic and ileal samples followed a modified method previously described by Matyash et al [38]. Colonic and ileal contents were weighed and transferred separately to sterile ceramic bead tubes (NucleoSpin® Bead Tubes, Macherey-Nagel, Dueren, Germany). Initially, 194 µL of cold MeOH was added to each weighed sample and vortexed for 10 s. Subsequently, 645 µL of cold MTBE was added, and the samples were vigorously vortexed. Homogenization and extraction were performed using a Precellys® Evolution Homogenizer (Bertin Corp., Rockville, Maryland, USA) at 4,500 rpm, with 3 cycles of 40 s each, with a 2 s pause between cycles. Following lysis, samples were shaken for an additional 20 min at 4 °C using a ThermoMixer (ThermoMixer® C, Eppendorf, Hamburg, Germany). Phase separation was achieved by adding 161 µL of H_2O and incubating for an additional 10 min, resulting in a total volume of 1 mL. The samples were then centrifuged for 10 min at 21,000 x g and 4 °C, and the upper phase was transferred to safety reaction tubes (Eppendorf, Hamburg, Germany). A pooled MTBE extract from colon or ileum extracts, was evaporated at 40 °C using a SpeedVac Concentrator (Savant SPD121P, Fisher Scientific, Waltham, MA, United States), and the residue was redissolved in an equivalent volume of ACN/iPrOH/H_2O (65/30/5) spiked with a mixture of stable isotope-labeled standards.

2.3. UHPLC-MS/MS conditions

Lipid standards and samples were analyzed using an ultrahigh-performance liquid chromatography system (ExionLC, AB Sciex LLC, Framingham, MA, USA) coupled to a quadrupole time-of-flight mass spectrometer (X500 QTOF MS, AB Sciex LLC, Framingham, MA, USA)

equipped with a DuoSpray ion source. Prior to each analysis, mass calibration was conducted in both ionization modes using a calibration delivery system (ESI Positive/Negative Calibration Solution for X500, AB SCIEX Germany GmbH, Darmstadt, Germany). The QTOF mass spectrometer was automatically recalibrated between the runs after every tenth injection. For the MS/MS method, the information dependent acquisition (IDA) mode was employed. Biological samples and standard mixtures were analyzed in full-scan mode (100–1500 Dalton) in both positive (+) and negative (−) electrospray ionization modes, together with MS/MS IDA experiments. Details of the parameters set for the TOF MS and TOF MS/MS methods are summarized in Table S2. Five different RP columns, each with similar dimensions (150 mm x 2.1 mm, 1.6–1.8 µm) were compared. Following columns were used: ACQUITY™ Premier HSS T3 (150 mm × 2.1 mm, 1.8 µm), CORTECS® UPLC® C18 column (150 mm × 2.1 mm, 1.6 µm), ACQUITY™ Premier BEH C18 (150 mm × 2.1 mm, 1.7 µm), ACQUITY UPLC® BEH C18 (150 mm × 2.1 mm, 1.7 µm) and ACQUITY UPLC® BEH C8 (150 mm × 2.1 mm, 1.7 µm), purchased from Waters (Milford, MA, USA). Elution of lipids was ensured by a mobile phase A of 60:40 ACN/H_2O, and mobile phase B, composed of 90:10 iPrOH/ACN. We investigated the influence of different modifiers on the separation efficiency through eight conditions, including (1) 10 mM ammonium acetate (pH = 6.7); (2) 10 mM ammonium acetate with acidification (0.1 % acetic acid) (pH = 4.5); (3) 5 mM ammonium acetate (pH = 6.7); (4) 5 mM ammonium acetate with acidification (0.1 % acetic acid) (pH = 4.2); (5) 10 mM ammonium formate (pH = 6.4); (6) 10 mM ammonium formate with acidification (0.1 % formic acid) (pH = 3.2); (7) 5 mM ammonium formate (pH = 6.4) and (8) 5 mM ammonium formate with acidification (0.1 % formic acid) (pH = 3.0). The chromatographic conditions included a flow rate of 0.25 mL/min, and the run started with an isocratic step of 1.5 min with 32 % B. This was followed by a gradual increase to 97 % B until 21 min, maintained for 4 min, and returned to initial conditions in 0.1 min. Five microliters of sample were injected, and the column oven temperature was set to 40 °C. Prior to sample analysis, blanks spiked with a mix of internal standards were injected in triplicate to monitor retention time and intensity drifts. Precision was assessed by calculating the percentage of coefficient of variation (CV%).

2.4. Data processing and analysis

Targeted peak picking was conducted using Sciex OS Analytics 3.0 (AB Sciex LLC, Framingham, MA, USA), where retention time, peak width and tailing factor were extracted. For non-targeted peak picking, Genedata Expressionist Refiner MS 15.0.7 (Genedata GmbH, Basel, Switzerland) was employed. The processing of.wiff2 data included several steps such as chemical noise subtraction, griding, retention time restriction, chromatogram peak detection, blank peak filter, chromatogram isotope clustering, intensity filter, MS/MS consolidation, and MS/MS peak detection. These processing steps generated a data matrix containing features defined by a unique cluster number (mass-to-charge ratio (m/z) and retention time) along with the maximum intensity values observed for each sample. MZmine software version 3.9.0 was employed for visualization of extracted ion chromatograms by exporting.wiff2 to mzML files with ProteoWizard msConvert 3.0.20342 [39,40]. To annotate MS/MS associated with the generated clusters, MSPepSearch (released at 02/22/2019) was used to match experimental MS/MS spectra against MS-DIAL-TandemMassSpectralAtlas-VS69 library (0.01 of precursor ion m/z uncertainty and 0.05 of ms peak m/z uncertainty) [41]. Matches with dot product over 600 were considered for further in-depth elucidation and identification. CANOPUS from Sirius 5.8.5 was employed for lipid classification and the prediction of known and unknown features [42–44].

3. Results and discussion

In this study, we evaluated the performance of five RP columns across eight buffer conditions. We included ammonium acetate (AmAc) and ammonium formate (AmF) of 5 or 10 mM, with or without the addition of 0.1 % acetic or formic acid. We examined columns of ethylene bridged hybrid, hybrid surface technologies and core–shell with identical dimensions (150 mm × 2.1 mm) and particle size ranging from 1.6 to 1.8 µm. Our targeted analysis covered 140 lipid standards, consisting mainly of fatty acyls, sphingolipids, and glycerophospholipids analyzed under 40 different chromatographic conditions. Non-targeted lipidomics was performed on ileal and colonic content of OMM^{12} mice, employing a total of eight chromatographic conditions in positive and negative electrospray ionization mode (+/-ESI).

3.1. Evaluation of the RP conditions using standards

3.1.1. Reproducibility of RT and peak areas using lipid standards

Retention time variation and reproducibility of peak areas were monitored across every column and mobile phase combination by replicate injections of blank samples spiked with four deuterated lipids, analyzed in ESI(+) RPLC-MS. For peak areas, the lowest average CV% (0.6 %) was observed with 5 mM AmF + 0.1 % formic acid on the BEH C18 HST (Fig. S1A). The BEH C18 HST with either 5 mM AmF or AmAc without acidification exhibited the lowest average CV% (<0.1 %) for retention time (Fig. S1B). In contrast, the Cortecs C18 column showed the highest CV% values for both peak areas (~7%) and retention times (~0.8 %) compared with other RP columns (Fig. S1A–B).

3.1.2. Selection of mobile phase modifiers

We conducted a systematic evaluation of eight buffer conditions to assess their impact on the peak areas of lipid standards. For ESI(−), we observed a significant increase in sensitivity for most lipid classes when using 5 mM AmAc (Fig. 1A-B). Specifically, when comparing AmAc to AmF at both concentrations, a fivefold increase in the peak area of fatty acids, such as palmitoleic acid, was prominent (Fig. S3A). Furthermore, employing 5 mM AmAc instead of 10 mM improved lipid ionization efficiency, particularly in peak areas of phosphatidylglycerols (PG) and PA. Lower buffer concentrations resulted in a fivefold increase in peak areas for N-acyl amines (Fig. S2B-G). In ESI(+) mode, 5 mM AmF, both with and without acidification, demonstrated superior performance compared to 5 mM AmAc for most lipids, with higher peak areas of fatty acyls and phosphatidylcholines (PC) (Fig. 1C-D & Fig. S3B). Moreover, employing 5 mM AmF instead of 10 mM resulted in improved peak areas for various lipid species, for example PG (Fig. S2E). Interestingly, similar results were achieved in both ESI modes for three lipid classes employing the same additive type (Fig. 1E–F & Fig. S2H). In particular, the use of 5 mM AmAc without acidification resulted in higher peak areas for Cer and PE, whereas acidification of 5 mM AmAc resulted in higher peak areas for PS. All columns exhibited similar behavior, with higher peak areas for most lipids using 5 mM AmAc in ESI(−) or 5 mM AmF in ESI(+). Our findings align with previous studies, indicating the preference for ammonium acetate in ESI(−) to enhance lipid ionization efficiency [28]. This preference is attributed to the higher pH values achieved by AmAc compared to AmF, leading to increased deprotonation efficiency of lipid species [45]. Interestingly, although 5 mM AmAc resulted in a 0.02 pH unit lower than 10 mM AmAc, the lower AmAc concentration consistently exhibited higher signal areas for most lipid standards. This observation may be attributed to a potential suppression effect associated with higher salt concentrations [46].

3.1.3. Selection of RP columns

Since peak areas of lipid standard remained unaffected by column technologies (Fig. 1A-F), we calculated the average of key chromatographic parameters across eight buffer conditions for HSS T3 HST, Cortecs C18, BEH C18 HST, BEH C18, and BEH C8. Parameters included peak width and tailing factor. Notably, BEH C18 HST consistently outperformed the other columns under the same conditions, showcasing superior performance, particularly for lipids with amine or hydroxy

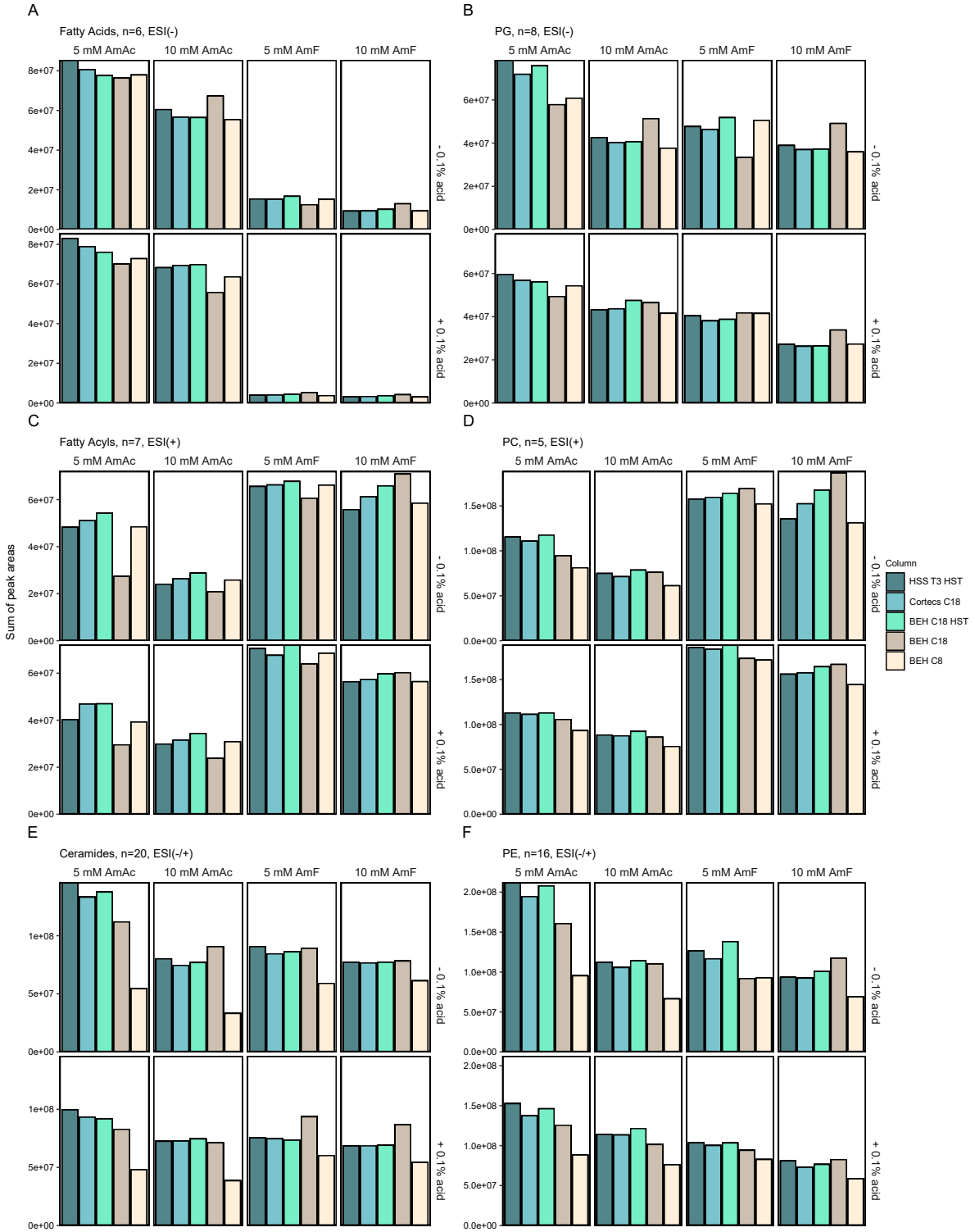

Fig. 1. The impact of two ammonium-based buffers (AmAc and AmF) at 5 and 10 mM and mobile phase acidification ((+/-) 0.1 % acid) on ionization efficiency expressed by summed peak areas per condition of selected lipid standards. Lipid classes including fatty acids (n = 6) and PG (n = 8) in ESI(−) (A-B), fatty acyls (n = 7) and PC (n = 5) in ESI(+) (C-D) or ceramides (n = 20) and PE (n = 16) in both modes (ESI(−/+) (E-F) were analyzed with five columns. Legend: AmAc: ammonium acetate and AmF: ammonium formate. Acetic acid (0.1 %) was added to 5 or 10 mM AmAc while formic acid (0.1 %) was used with 5 or 10 mM AmF.

head groups (Fig. 2A–B). BEH C18 HST resulted in better peak shapes, reduced peak width, and minimized tailing factor for a variety of lipid species (Fig. S3C-D). Specifically, the HST technology reduced peak tailing by 40 % for PS lipids compared to core–shell technology and by 20 % for conventional columns. Moreover, a 40 % reduction in tailing factors was observed for PC compared to the other technologies. The peak widths of PA lipids were reduced by 20 % using the HST column compared to the conventional one. As reported in the literature [23], particularly acidic phospholipids, mainly PA and PS, tend to elute in broad peaks, making their peak detection challenging in lipidomics. Our comparison under various buffer conditions and column technologies confirmed an improvement in the detection of PA, PS and other lipid

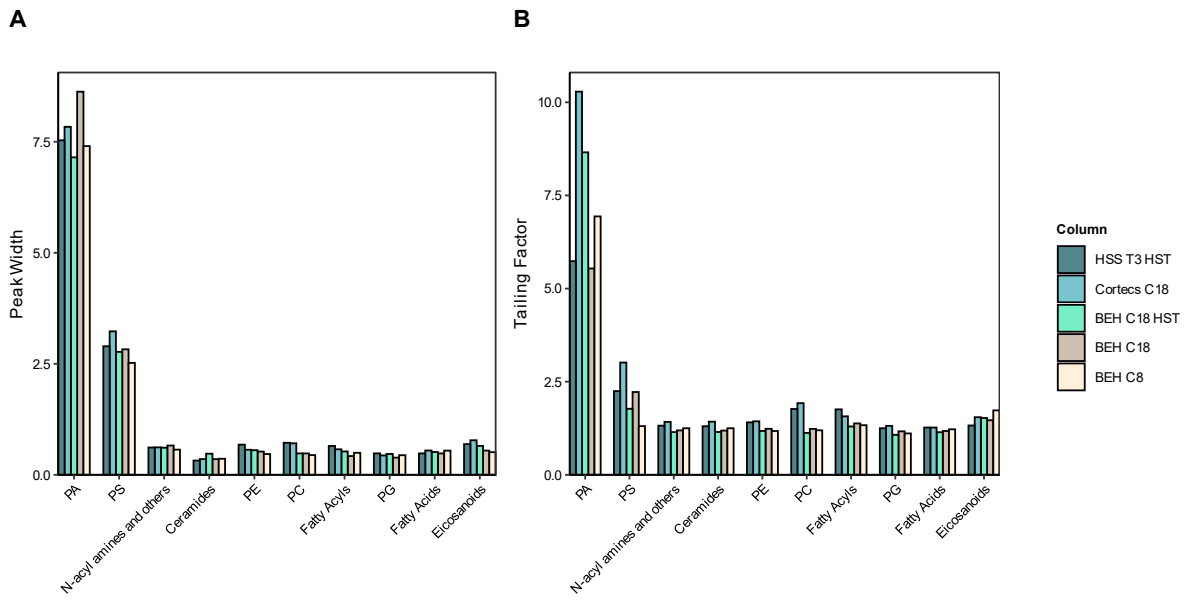

Fig. 2. Average of peak widths (A) and tailing factors (B) evaluated on ten different lipid classes detected in ESI(+/-) and separated on five different columns including HSS T3 HST, Cortecs C18, BEH C18 HST, BEH C18 and BEH C8. Lipid classes included PA (n = 2), PS (n = 1), N-acyl amines and others (n = 6), ceramides (n = 14), PE (n = 16), PC (n = 5), fatty acyls (n = 14), PG (n = 9), fatty acids (n = 7) and eicosanoids (n = 2).

species using HST technology compared to conventional one.

3.2. Non-targeted lipidomics for selection of mobile phase modifiers

Our next step was to profile the intestinal lipidome of the OMM[12] mouse model, by analyzing the content of ileum and colon sections of the gut. Therefore, we conducted a similar approach on intestinal samples as described above by comparing eight mobile phase modifiers, only using the superior BEH C18 HST technology. We revealed that in ESI(−), the use of 5 mM AmAc without acetic acid outperforms consistently all other buffer conditions in terms of number of detected features (MS1), features with MS/MS (MS2), and number of identified lipids (ID) in colonic and ileal samples (Fig. 3A & Fig. S4A). In particular, 5 mM AmAc resulted in around 2 times more detected features (100 %) than 5 mM AmF. Additionally, we observed a 72 % increase in the total count of identified features (dot product > 600) when using 5 mM AmAc compared to 10 mM AmAc. In ESI(+), we did not observe a substantial effect on the count of detected features, number of MS/MS or identification rate. We employed CANOPUS for classification of MS/MS features. In ESI(−), 5 mM AmAc exhibited the highest number of classified features, showing approximately 4.5 times increase in feature classification compared to 5 mM AmF in both colon and ileum samples (Fig. 3B & Fig. S4B). However, AmF and AmAc used at 5 or 10 mM concentrations showed similar feature counts and classification rates in ESI(+). We further compared the overall count of common lipid species classified using the MS-DIAL library in both ESI modes across eight buffer conditions [41]. The use of 5 mM AmAc resulted in improved coverage of nine lipid classes in both colon and ileum samples, mainly Cer, ether-linked PE, and ether-linked monogalactosyldiacylglycerols (MGDG, ether), in ESI(−) (Fig. 3C & Fig. S4C). On the other hand, 5 mM AmF in ESI(+) resulted in higher count of specific classes, mainly diacylglycerols (DG) and triacylglycerols (TG). We also ranked the relative maximum signal intensities for each lipid class across all buffer conditions of selected lipids detected in both ileal and colonic samples (Fig. 3D & Fig. S4D). In ESI(−), 5 mM AmAc without acidification showed the highest maximum intensities for most selected lipid classes, followed by 10 mM AmAc and 5 mM AmAc with 0.1 % acetic acid. Notably, the use of AmF with both concentrations as an additive resulted in very poor signal intensity for certain lipid classes, including Cer, fatty amides and glycosyldiradylglycerols (DGDG). For ESI(+), 5 mM AmF and AmAc performed the best, yielding the highest intensities for most selected lipid classes. AmF showed sufficient to excellent peak heights (90 %) for diverse lipid classes, such as lysophosphatidylcholines (LPC), cholesteryl esters (CE), and sphingomyelins (SM). On the other hand, AmAc demonstrated better ionization efficiency for different derivatives of Cer and sterol lipids, detected in colon and ileum samples (Fig. 3D & Fig. S4D). These observations are in line with previous studies showcasing the better performance of AmAc in ESI(−) and AmF in ESI(+), but decreasing the salt concentration to 5 mM [28,47].

4. Conclusion

In the present study, we assessed various mobile phase modifiers and column technologies for lipid analysis in both simple and complex matrices. Our findings emphasize the importance of considering multiple factors when comparing columns and additives in LC-MS analysis of lipid species. Hybrid surface technology columns outperformed other technologies, by reducing peak width and tailing factor for various lipid classes. HST columns showed increased sensitivity and better coverage for diverse lipid species such as sphingolipids, PA, and PS. Our targeted and non-targeted lipidomics approaches yielded similar results in the evaluation of mobile phase modifiers. Specifically, 5 mM AmAc without acidification demonstrated better results in ESI(−), providing higher signal intensity, increased coverage, and efficient lipid classification and identification compared to other additives. In ESI(+), both 5 mM AmF and AmAc exhibited comparable results, showcasing robust signal intensities for common lipids and enhanced coverage for various lipid species in both sample types.

CRediT authorship contribution statement

Habiba Selmi: Writing – original draft, Visualization, Methodology, Investigation, Data curation, Conceptualization. **Alesia Walker:** Writing – review & editing, Visualization, Validation, Supervision, Funding acquisition, Conceptualization. **Laurent Debarbieux:** Writing – review & editing, Supervision, Funding acquisition, Conceptualization. **Philippe Schmitt-Kopplin:** Writing – review & editing, Supervision, Funding acquisition, Conceptualization.

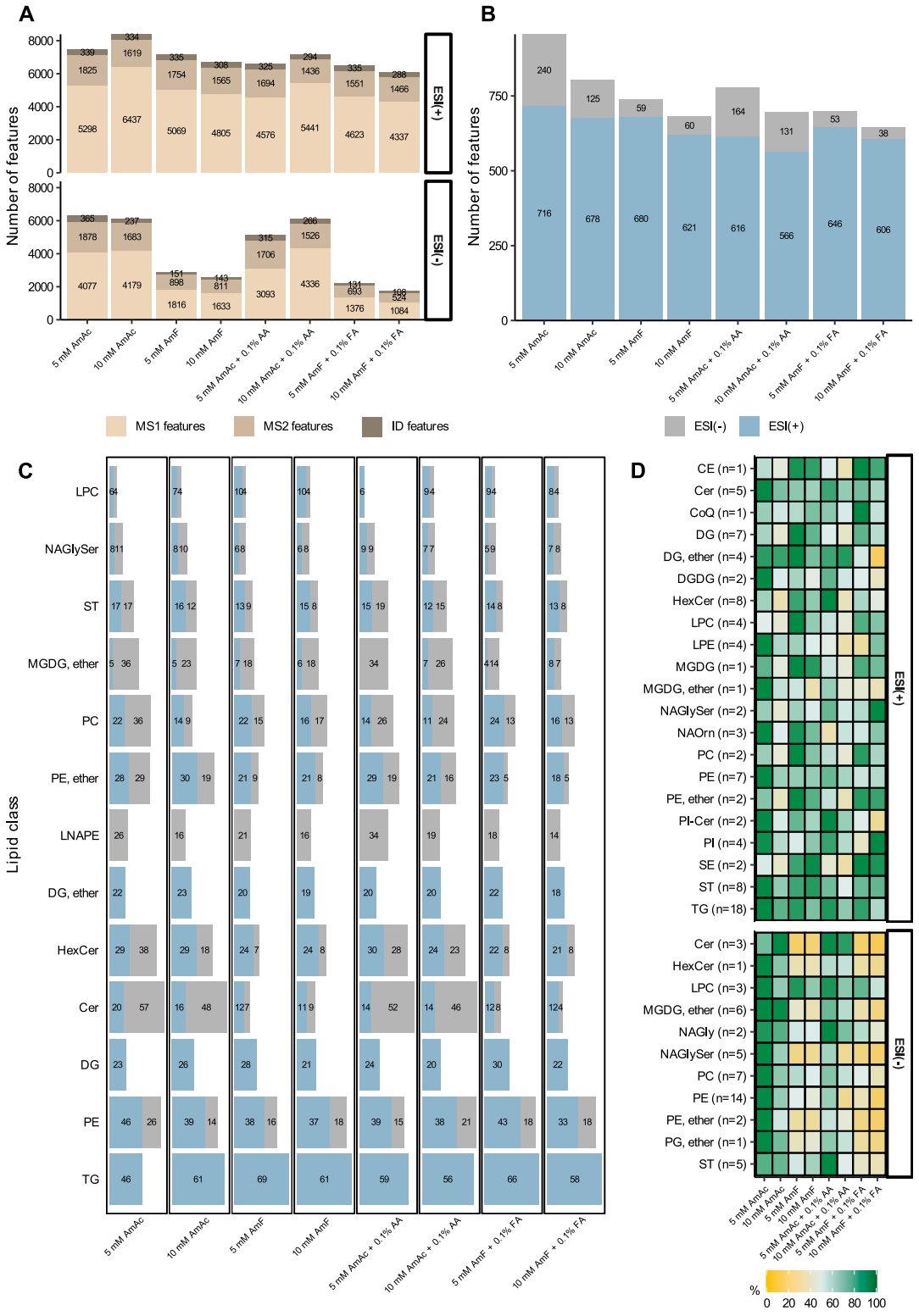

Fig. 3. The impact of various mobile phase modifiers on feature coverage, lipid classification and the ionization efficiency in a pooled colon sample analyzed with LC-MS/MS in ESI(+/-). Intestinal lipids were separated using the BEH C18 HST column. (A) Bar plots showing the total number of detected features (MS1), features with MS2 and features annotated by the MS-DIAL library (ID). (B) Bar plots representing the total count of classified features (probability over 0.6) by CANOPUS. (C) Bar plots showing the individual count of common lipid classes among different buffer additives. (D) Heatmap showing the percentage of relative peak intensities, for lipid classes detected under all eight buffer conditions in ESI(+/-). The percentages of each common lipid species were defined to the highest peak intensity set to 100 %, across the eight buffer conditions. Peak intensities of lipid classes were categorized as follows: moderate poor (<50 %), sufficient (≥50 %), and excellent (≥80 %). Legend: AmAc: ammonium acetate; AmF: ammonium formate, AmAc + 0.1 % AA: ammonium acetate and 0.1 % acetic acid; AmF + 0.1 % FA: ammonium formate and 0.1 % formic acid.

Declaration of competing interest

The authors declare that they have no known competing financial interests or personal relationships that could have appeared to influence the work reported in this paper.

Data availability

Data will be made available on request.

Acknowledgements

This research was funded by the DFG project number 446067148 (PhaStGut) to AW and from PRCI ANR-20-CE92-0048 (PhaStGut) to LD. We thank Thierry Pedron for his help in collecting intestinal samples from mice.

Appendix A. Supplementary material

Supplementary material to this article can be found online at https://doi.org/10.1016/j.jchromb.2024.124188.

References

[1] H. Matthews, J. Hanison, N. Nirmalan, "Omics"-informed drug and biomarker discovery: opportunities, challenges and future perspectives, Proteomes 4 28 (2016), https://doi.org/10.3390/proteomes4030028.
[2] E.A. Dennis, Lipidomics joins the omics evolution, Proc. Natl. Acad. Sci. U.S.A. 106 (2009) (2009) 2089–2090, https://doi.org/10.1073/pnas.0812636106.
[3] M.R. Wenk, The emerging field of lipidomics, Nat. Rev. Drug Discov. 4 (2005) 594–610, https://doi.org/10.1038/nrd1776.
[4] E.M. Storck, C. Özbalci, U.S. Eggert, Lipid cell biology: a focus on lipids in cell division, Annu. Rev. Biochem. 87 (2018) 839–869, https://doi.org/10.1146/annurev-biochem-062917-012448.
[5] A. Shevchenko, K. Simons, Lipidomics: coming to grips with lipid diversity, Nat. Rev. Mol. Cell Biol. 11 (2010) 593–598, https://doi.org/10.1038/nrm2934.
[6] G. Di Paolo, T.-W. Kim, Linking lipids to Alzheimer's disease: cholesterol and beyond, Nat. Rev. Neurosci. 12 (2011) 284–296, https://doi.org/10.1038/nrn3012.
[7] K. Honda, D.R. Littman, The microbiota in adaptive immune homeostasis and disease, Nature 535 (2016) 75–84, https://doi.org/10.1038/nature18848.
[8] M. Bae, et al., Akkermansia muciniphila phospholipid induces homeostatic immune responses, Nature 608 (2022) 168–173, https://doi.org/10.1038/s41586-022-04985-7.
[9] E.M. Brown, et al., Bacteroides-derived sphingolipids are critical for maintaining intestinal homeostasis and symbiosis, Cell Host & Microbe 25 (2019) 668–680, https://doi.org/10.1016/j.chom.2019.04.002.
[10] S. Bang, et al., A cardiolipin from *muribaculum intestinale* induces antigen-specific cytokine responses, J. Am. Chem. Soc. 145 (2023) 23422–23426, https://doi.org/10.1021/jacs.3c09734.
[11] E. Fahy, et al., Update of the LIPID MAPS comprehensive classification system for lipids, J. Lipid Res. 50 (2009) S9–S14, https://doi.org/10.1194/jlr.R800095-JLR200.
[12] E. Fahy, D. Cotter, M. Sud, S. Subramaniam, Lipid classification, structures and tools, *Biochimica et Biophysica Acta (BBA) - Molecular and Cell Biology of Lipids* 1811 (2011) 637–647, https://doi.org/10.1016/j.bbalip.2011.06.009.
[13] T. Cajka, O. Fiehn, Comprehensive analysis of lipids in biological systems by liquid chromatography-mass spectrometry, TrAC Trends Anal. Chem. 61 (2014) 192–206, https://doi.org/10.1016/j.trac.2014.04.017.
[14] E.-M. Harrieder, F. Kretschmer, S. Böcker, M. Witting, Current state-of-the-art of separation methods used in LC-MS based metabolomics and lipidomics, J. Chromatograp. B 1188 (2022) 123069, https://doi.org/10.1016/j.jchromb.2021.123069.
[15] K. Sandra, P. Sandra, Lipidomics from an analytical perspective, Curr. Opin. Chem. Biol. 17 (2013) 847–853, https://doi.org/10.1016/j.cbpa.2013.06.010.
[16] C.W.N. Damen, G. Isaac, J. Langridge, T. Hankemeier, R.J. Vreeken, Enhanced lipid isomer separation in human plasma using reversed-phase UPLC with ion-mobility/high-resolution MS detection, J. Lipid Res. 55 (2014) 1772–1783, https://doi.org/10.1194/jlr.D047795.
[17] P.A. Vorkas, et al., Untargeted UPLC-MS profiling pipeline to expand tissue metabolome coverage: application to cardiovascular disease, Anal. Chem. 87 (2015) 4184–4193, https://doi.org/10.1021/ac503775m.
[18] P. Žuvela, et al., Column characterization and selection systems in reversed-phase high-performance liquid chromatography, Chem. Rev. 119 (2019) 3674–3729, https://doi.org/10.1021/acs.chemrev.8b00246.
[19] H. Ogiso, T. Suzuki, R. Taguchi, Development of a reverse-phase liquid chromatography electrospray ionization mass spectrometry method for lipidomics, improving detection of phosphatidic acid and phosphatidylserine, Anal. Biochem. 375 (2008) 124–131, https://doi.org/10.1016/j.ab.2007.12.027.
[20] J.C. Heaton, D.V. McCalley, Some factors that can lead to poor peak shape in hydrophilic interaction chromatography, and possibilities for their remediation, J. Chromatograp. A 1427 (2016) 37–44, https://doi.org/10.1016/j.chroma.2015.10.056.
[21] K.T. Myint, T. Uehara, K. Aoshima, Y. Oda, Polar anionic metabolome analysis by nano-lc/ms with a metal chelating agent, Anal. Chem. 81 (2009) 7766–7772, https://doi.org/10.1021/ac901269h.
[22] D. Winter, J. Seidler, Y. Ziv, Y. Shiloh, W.D. Lehmann, Citrate boosts the performance of phosphopeptide analysis by UPLC-ESI-MS/MS, J. Proteome Res. 8 (2009) 418–424, https://doi.org/10.1021/pr800304n.
[23] O.L. Knittelfelder, B.P. Weberhofer, T.O. Eichmann, S.D. Kohlwein, G. N. Rechberger, A versatile ultra-high performance LC-MS method for lipid profiling, J. Chromatograp. B 951–952 (2014) 119–128, https://doi.org/10.1016/j.jchromb.2014.01.011.
[24] J.C. Lee, Y.B. Kim, M.H. Moon, Enhancement of acidic lipid analysis by nanoflow ultrahigh performance liquid chromatography–mass spectrometry, Analytica Chimica Acta 1166 (2021) 338573, https://doi.org/10.1016/j.aca.2021.338573.
[25] R.S. Plumb, et al., Hybrid organic/inorganic hybrid surface technology for increasing the performance of LC/MS(MS)-based drug metabolite identification studies: application to gefitinib and metabolites in mouse plasma and urine, J. Pharmaceutical Biomed. Anal. 200 (2021) 114076, https://doi.org/10.1016/j.jpba.2021.114076.
[26] M. DeLano, et al., Using hybrid organic-inorganic surface technology to mitigate analyte interactions with metal surfaces in UHPLC, Anal. Chem. 93 (2021) 5773–5781, https://doi.org/10.1021/acs.analchem.0c05203.
[27] G. Isaac, I.D. Wilson, R.S. Plumb, Application of hybrid surface technology for improving sensitivity and peak shape of phosphorylated lipids such as phosphatidic acid and phosphatidylserine, J. Chromatograp. A 1669 (2022) 462921, https://doi.org/10.1016/j.chroma.2022.462921.
[28] T. Cajka, O. Fiehn, Increasing lipidomic coverage by selecting optimal mobile-phase modifiers in LC–MS of blood plasma, Metabolomics 12 (2016) 34, https://doi.org/10.1007/s11306-015-0929-x.
[29] L. Bojic, et al., Lipidome of atherosclerotic plaques from hypercholesterolemic rabbits, IJMS 15 (2014) 23283–23293, https://doi.org/10.3390/ijms151223283.
[30] J.M. Castro-Perez, et al., Comprehensive LC−MS ^{E} Lipidomic analysis using a shotgun approach and its application to biomarker detection and identification in osteoarthritis patients, J. Proteome Res. 9 (2010) 2377–2389, https://doi.org/10.1021/pr901094j.
[31] S. Chen, et al., Effect of Allium macrostemon on a rat model of depression studied by using plasma lipid and acylcarnitine profiles from liquid chromatography/mass spectrometry, J. Pharmaceutical Biomed. Anal. 89 (2014) 122–129, https://doi.org/10.1016/j.jpba.2013.10.045.
[32] S. Chen, et al., Serum lipid profiling of patients with chronic hepatitis B, cirrhosis, and hepatocellular carcinoma by ultra fast LC/IT-TOF MS: liquid phase separations, Electrophoresis 34 (2013) 2848–2856, https://doi.org/10.1002/elps.201200629.
[33] L. Whiley, J. Godzien, F.J. Ruperez, C. Legido-Quigley, C. Barbas, In-vial dual extraction for direct lc-ms analysis of plasma for comprehensive and highly reproducible metabolic fingerprinting, Anal. Chem. 84 (2012) 5992–5999, https://doi.org/10.1021/ac300716u.
[34] M. Giera, et al., Lipid and lipid mediator profiling of human synovial fluid in rheumatoid arthritis patients by means of LC–MS/MS. *Biochimica et Biophysica Acta (BBA), Mol. Cell Biol. Lipids* 1821 (2012) 1415–1424, https://doi.org/10.1016/j.bbalip.2012.07.011.
[35] C. Eberl, et al., Reproducible colonization of germ-free mice with the oligo-mouse-microbiota in different animal facilities, Front. Microbiol. 10 (2020) 2999, https://doi.org/10.3389/fmicb.2019.02999.
[36] Q. Lamy-Besnier, R. Koszul, L. Debarbieux, M. Marbouty, Closed and high-quality bacterial genome sequences of the oligo-mouse-microbiota community, Microbiol. Resour. Announc. 10 (2021), https://doi.org/10.1128/MRA.01396-20.
[37] J. Elzinga, J. Van Der Oost, W.M. De Vos, H. Smidt, The use of defined microbial communities to model host-microbe interactions in the human gut, Microbiol. Mol. Biol. Rev. 83 (2019), https://doi.org/10.1128/MMBR.00054-18.
[38] V. Matyash, G. Liebisch, T.V. Kurzchalia, A. Shevchenko, D. Schwudke, Lipid extraction by methyl-tert-butyl ether for high-throughput lipidomics, J. Lipid Res. 49 (2008) 1137–1146, https://doi.org/10.1194/jlr.D700041-JLR200.
[39] R. Schmid, et al., Integrative analysis of multimodal mass spectrometry data in MZmine 3, Nat. Biotechnol. 41 (2023) 447–449, https://doi.org/10.1038/s41587-023-01690-2.
[40] M.C. Chambers, et al., A cross-platform toolkit for mass spectrometry and proteomics, Nat. Biotechnol. 30 (2012) 918–920, https://doi.org/10.1038/nbt.2377.
[41] H. Tsugawa, et al., A lipidome atlas in MS-DIAL 4, Nat. Biotechnol. 38 (2020) 1159–1163, https://doi.org/10.1038/s41587-020-0531-2.
[42] K. Dührkop, et al., SIRIUS 4: a rapid tool for turning tandem mass spectra into metabolite structure information, Nat. Methods 16 (2019) 299–302, https://doi.org/10.1038/s41592-019-0344-8.
[43] K. Dührkop, et al., Systematic classification of unknown metabolites using high-resolution fragmentation mass spectra, Nat. Biotechnol. 39 (2021) 462–471, https://doi.org/10.1038/s41587-020-0740-8.
[44] K. Dührkop, H. Shen, M. Meusel, J. Rousu, S. Böcker, Searching molecular structure databases with tandem mass spectra using CSI:FingerID, Proc. Natl. Acad. Sci. U.S.A. 112 (2015) 12580–12585, https://doi.org/10.1073/pnas.1509788112.

[45] J.R. Kanicky, D.O. Shah, Effect of degree, type, and position of unsaturation on the pKa of long-chain fatty acids, J. Colloid Interf. Sci. 256 (2002) 201–207, https://doi.org/10.1006/jcis.2001.8009.
[46] T.L. Constantopoulos, G.S. Jackson, C.G. Enke, Effects of salt concentration on analyte response using electrospray ionization mass spectrometry, J. Am. Soc. Mass Spectrom. 10 (1999) 625–634, https://doi.org/10.1016/S1044-0305(99)00031-8.
[47] T. Cajka, et al., Optimization of mobile phase modifiers for fast LC-MS-based untargeted metabolomics and lipidomics, IJMS 24 (2023) 1987, https://doi.org/10.3390/ijms24031987.